

## Numerical Simulation of Pig Motion through Gas Pipelines

S.M. Hosseinalipour<sup>1</sup>, A. Zarif Khalili<sup>1</sup>, and A. Salimi<sup>1</sup>

<sup>1</sup> CAE Center, CFD Lab, Mechanical Engineering Department  
 Iran University of Science and Technology, Narmak, Tehran, Iran  
 alireza.zarif@gmail.com

### Abstract

Pigs are utilized in pipelines to perform operations such as dewatering, cleaning, and internal inspection for damages. Transient motion of pigs through gas pipelines has been simulated numerically in order to help engineers predict the variables related to pig motion such as estimating its speed, required driving pressure, and the amount of fluid bypass through the pig. In this paper, the continuity and linear momentum equations for compressible gas flows were discretized by finite difference method based on moving and staggered grids. These equations were solved together with dynamic equation for pig movement and the equation for modeling bypass flow. Besides, gas was considered both ideal and real. Test cases representing typical pigging operations in pipelines with or without flanges and branches were studied using the numerical model developed. The fluid flow and pig behavior predicted by the model have a reasonable behavior.

### Introduction

A large variety of pigs has now evolved to perform operations such as cleaning out deposits and debris, locating obstructions, liquid and gas removal, and internal inspection for damage or corrosion spots in pipelines. Pigging helps keep the pipeline free of liquid, reducing the overall pressure drop, and thereby increasing the pipeline flow efficiency.

Pipeline pigs may be broken down into two fundamental groups: conventional pigs, which perform a function such as cleaning or dewatering, and intelligent pigs, which provide information about the condition of a pipeline. All intelligent pigs need a clean line for optimum performance, and this requires the development of highly effective conventional pigs and pigging programs. Engineers have to consider many parameters for designing a pigging operation such as the effects of velocity, and determination of optimum pig speeds; design of pigs capable of performing in widely differing diameters; the effects of by-pass and optimum by-pass configuration; the effects of the differential pressures across the seals. However, most of the available knowledge is based on field experience. Hence, selecting the best pig, often involves some guesswork, and, consequently, a high degree of uncertainty.

The speeds recommended for routine, conventional, on-stream pigging are 1 to 5m/sec for liquid lines and 2 to 7m/sec in gas lines [1]. Good estimations of pig velocity and the time pig reaches the end of pipeline will help engineers design and perform a suitable pigging operation.

We can find very few papers dealing with the numerical simulation of pig motion in gas and liquid pipelines. Sullivan [2], Haun [3], treat the dynamics of simplified pigs in gas lines. Short [4] conducted an experimental research program aimed at the understanding of the fundamental problems related to pipeline pigging. A simple model to predict the pig motion driven by incompressible fluids under steady-state conditions was presented by Azevedo et al. [5]. Vianes Campo and Rachid [6] studied the dynamics of pigs through

pipelines using the method of characteristics. Recently, Nieckele et al. [7] investigated isothermal pigging operations through gas and liquid pipelines. In addition, the contact forces developed by disk pigs and the pipe wall were predicted by a post-buckling finite element analysis of the discs.

This paper deals with simulation and modeling of pigs through gas pipelines. The equations governing the conservation of mass, linear momentum for the fluid were numerically solved by a finite difference method based on staggered moving grids these equations were coupled with an equation that describes the pig dynamics. Mathematical model for the prediction of the bypass flow through pigs was based on Nieckele et al. [7]. In order to simulate more realistic pigging operations, pigging under high pressures around 90 bars and the deviation from ideal gas law was investigated. Gas consumption through pipeline branches was also considered.

### Governing Equations

Equations of mass, momentum, state and dynamic of pig are solved simultaneously. The flow is considered to be isothermal. Fig. 1 represents an elementary section of a variable area duct. The centerline of the duct is inclined with the horizontal at an angle  $\beta$ . It is assumed that the area change over the length  $dx$  is small, so the flow is essentially one-dimensional. The density, velocity, pressure and area are, respectively,  $\rho$ ,  $V$ ,  $P$ ,  $A$ . The acceleration of gravity vector is represented by  $g$ , and  $\tau_s$  is the viscous stress acting at the wall.

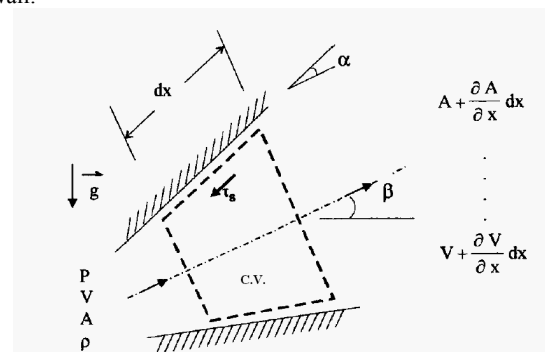


Figure 1. Control volume for one-dimensional flow analysis

For the control volume of Fig. 1, the mass conservation equation can be written as  $(\partial m_{c.v.}/\partial t) = \dot{m}_{in} - \dot{m}_{out}$ , where  $m_{c.v.} = \rho A dx$  is the mass of fluid in the control volume and  $\dot{m}$  is the mass flux through the boundaries. Thus, the continuity equation can be written in the following form:

$$\frac{\partial(\rho A dx)}{\partial t} = \rho AV - \left[ \left( \rho + \frac{\partial \rho}{\partial x} dx \right) \left( A + \frac{\partial A}{\partial x} dx \right) \left( V + \frac{\partial V}{\partial x} dx \right) \right] \quad (1)$$

Neglecting higher order derivatives and using the definition of material derivative, Eq. (1) can be rearranged in the following form:

$$\frac{1}{A} \frac{DA}{Dt} + \frac{1}{\rho} \frac{D\rho}{Dt} + \frac{\partial V}{\partial x} = 0 \quad (2)$$

where  $\frac{D}{Dt} = \frac{\partial}{\partial t} + V \frac{\partial}{\partial x}$

It should be noted that when gas pressure is high, pipe deformation is not negligible. In that case, the effects of pipe deformation due to pressure variations along the flow will be incorporated in the mass conservation equation (2). Considering the pipe as a cantilever beam, we can relate pipe's area change to its properties by the following relation (see Wylie and Streeter [8]):

$$\frac{1}{A} \frac{DA}{Dt} = \frac{D(1-\nu^2)}{eE} \frac{DP}{Dt} + V \frac{\partial A}{\partial x} \quad (3)$$

where  $e$  is the pipe wall thickness,  $E$  the Young modulus of elasticity of the pipe material, and  $\nu$  the Poisson ratio. Isothermal bulk modulus of the fluid is defined as  $K = \rho(\partial P/\partial \rho)_T$ , rearranging this equation we have:

$$\frac{1}{K} \frac{DP}{Dt} = \frac{1}{\rho} \frac{D\rho}{Dt} \quad (4)$$

Substituting equations (3) and (4) into Eq. (2), one obtains:

$$\frac{\partial P}{\partial t} + V \frac{\partial P}{\partial x} + \frac{K}{\xi} \frac{\partial V}{\partial x} + \frac{K}{\xi} \frac{V}{A} \frac{\partial A}{\partial x} = 0 \quad (5)$$

where  $\xi = 1 + KD(1-\nu^2)/(eE)$ .

In practical pigging operations, it is usual to have local gas consumption through some of the branches of the pipeline. In order to model this situation, a sink term can be considered in the continuity equation (5) at the location of each branch that diverts gas from the main line. The momentum conservation equation can be written as

$$\frac{\partial}{\partial t} (\dot{m}V)_{c.v.} = (\dot{m}V)_{in} - (\dot{m}V)_{out} + F_x \quad (6)$$

where  $(\dot{m}V)$  is the momentum efflux through the boundaries. Substituting proper relations for the terms of Eq. (6) and neglecting higher order derivatives, we have:

$$\frac{\partial(\rho V)}{\partial t} + \frac{\partial(\rho V^2)}{\partial x} = -\frac{\partial P}{\partial x} - \tau_s \left( \frac{P_m}{A} \right) \cos \alpha - \rho g \sin \beta - \frac{(P + \rho V^2)}{A} \frac{\partial A}{\partial x} \quad (7)$$

where  $P_m$  is the wet perimeter of the control volume section. The viscous force can be written in terms of a hydrodynamic friction coefficient  $f$ , and assuming  $\cos \alpha \approx 1$ , the linear momentum equation becomes:

$$\frac{\partial(\rho V)}{\partial t} + \frac{\partial(\rho V^2)}{\partial x} = -\frac{\partial P}{\partial x} - \frac{f}{2} \frac{\rho |V| V}{D} - \rho g \sin \beta - \frac{(P + \rho V^2)}{A} \frac{\partial A}{\partial x} \quad (8)$$

where  $f$ , the hydrodynamic friction coefficient, depends on the Reynolds number,  $Re = \rho |V| D / \mu$ , and, in the turbulent regime, also on the pipe relative roughness  $\varepsilon/D$ . The friction coefficient was evaluated by assuming fully developed flow.

Thus, for a laminar regime,  $Re < 2300$ , it was specified as  $f = 64/Re$ , while for the turbulent regime,  $Re \geq 2300$ , the friction factor was approximated by Miller's correlation (Fox and McDonald [9]),  $f = 0.25 \left\{ \log \left[ \frac{\varepsilon/D}{3.7} + \frac{5.74}{Re^{0.9}} \right] \right\}^{-2}$ . Using continuity equation (2) for the left hand side of Eq. (8) in conjunction with equation Eq. (3), we have:

$$\frac{\partial V}{\partial t} + V \frac{\partial V}{\partial x} - V \eta \frac{\partial P}{\partial t} + \frac{(1-\rho \nu^2 \eta)}{\rho} \frac{\partial P}{\partial x} + \frac{f |V| V}{2D} + g \sin \beta + \frac{P}{\rho A} \frac{\partial A}{\partial x} = 0 \quad (9)$$

where  $\eta = \frac{D(1-\nu^2)}{eE} \approx 0$ .

The coupling of the pig motion with the fluid flow in the pipeline was obtained through a balance of forces acting on the pig. The force balance on the pig can be written as:

$$m \frac{dV_{pig}}{dt} = (P_1 - P_2) A - mg \sin \beta - F_c \quad (10)$$

where  $V_{pig}$  is the pig velocity,  $m$  the pig mass,  $P_1$  and  $P_2$  the pressure on the upstream and downstream faces of the pig,  $\beta$  the angle of the pipe axis with the horizontal.

The term  $F_c$  represents the axial contact force between the pig and the pipe wall, acting in the direction of the pipe axis and opposing the pig's motion. The contact force can be allowed to vary along the pipe length. This variation may be caused by area changes along the pipe or due to changes in the pipe/pig friction coefficient. When the pig is not in motion, the contact force varies from zero to the maximum static force  $F_{stat}$ , in order to balance the pressure force due to the fluid flow. Once the pig is set in motion by the flow, the contact force assumes the constant value,  $F_{dyn}$ , representing the dynamic friction force that is generally different from the static force. In the present model, the contact force is considered as being independent of the pig velocity. The following relation relates the bypass flow to the pressure difference across the pig:

$$P_1 - P_2 = K_p \rho \frac{V_h^2}{2} \quad (11)$$

where  $K_p$  is the localized pressure drop coefficient and  $V_h$  is the fluid velocity at the bypass hole, measured relatively to the moving pig. Assuming the flow to be locally incompressible in the vicinity of the pig, a mass conservation equation can be written for a control volume moving with the pig. The pressure drop across the pig, can then be written as:

$$P_1 - P_2 = \frac{\rho K_p}{2} \left( \frac{A}{A_h} \right)^2 \left( \frac{Q}{A} - V_p \right)^2 \quad (12)$$

where  $A_h$  is the bypass hole cross sectional area. Note that  $Q/A$  is the average fluid velocity approaching the pig.

**Fluid Properties.** In addition to an ideal gas law for the density variation, a real gas model was employed. Equation of state for isothermal flow of an ideal gas is  $P = \rho (R_{gas} T_{ref})$ , where  $R_{gas}$  is the gas constant, and  $T_{ref}$  the reference temperature. Therefore, isothermal bulk modulus of gas will be equal to its pressure:

$$K = \rho(\partial P/\partial \rho)_T = P \quad (13)$$

For modeling flow of a real gas, density variations and isothermal bulk modulus of the fluid were calculated via

routines provided by NIST<sup>1</sup> Reference Fluid Thermodynamic and Transport Properties - REFPROP Version 7.0 (see [10]).

### Numerical Method

**Moving Grid.** Since the pig moves in the computational domain and both sides of the pig deforms with the pig movement, it is convenient to employ a coordinate system that stretches and contracts in the pipe, depending on the pig position.

The grid velocity  $v_g$  giving a regular numerical grid at each instant is defined by:

$$v_g(x,t) = \begin{cases} \frac{x}{X_{pig}} V_{pig}; & 0 \leq x \leq X_{pig} \\ \frac{(L-x)}{(L-X_{pig})} V_{pig}; & X_{pig} \leq x \leq L \end{cases} \quad (14)$$

where  $L$  is the pipe length,  $X_{pig}$  pig position, and  $x$  the position of each grid point.

The absolute velocity  $V$  is equal to  $\tilde{V} + v_g$  where  $\tilde{V}$  is the relative velocity. To transform the conservation equations, the convective fluxes  $V \frac{\partial}{\partial x}$  have to be replaced by  $\tilde{V} \frac{\partial}{\partial x}$ .

The set formed by equations (5), (9), (10) and (11), were discretized by a finite difference method. A staggered mesh distribution was selected to avoid unrealistic oscillatory solutions, as recommended by Patankar [11]. The equations were integrated in time using a fully implicit method and the space derivatives were approximated by the central difference method around the mesh point.

The resulting coefficient matrix is penta-diagonal. Since, the Thomas algorithm for tri-diagonal matrices (TDMA) can be extended to the solution of penta-diagonal systems, a direct penta-diagonal matrix algorithm (PDMA) described in [12] was used.

At each time step the set of equations were solved iteratively until convergent solutions were achieved. The iterations were terminated after overall accuracy had fallen below a tolerance. The time interval was sufficiently small to obtain solutions not influenced by the time step.

**Adaptive Mesh.** The total number of grid points inside the pipe was maintained constant in the numerical calculations of the flow field upstream and downstream of the pig. However, as the pig moved along the pipe, it was necessary to rearrange the node distribution. The number of grid points upstream and downstream of the pig was made proportional to the length of the pipe at each side of the pig. Note that when nodes had been transferred from downstream to upstream, all data for the grid points was interpolated before proceeding to the next time step. Further, the mesh was concentrated near the pig to better resolve the flow variables at this location.

### Pigging in a Gas Line with Flanges

The pipeline under consideration is 500 m long and horizontal. It is non-rigid with a reference diameter equal to 500 mm. It has two inward protruding flanges, located at 100 and 400 m from the inlet section of the pipe. The wall thickness  $e$  is 2.5 mm, and its roughness  $\epsilon$  is 0.05 mm. The pipe's Young modulus of elasticity,  $E$  is 200 GPa and its Poisson coefficient,  $\mu$  is 0.3.

At time equal to zero, air is pumped at the inlet, taking 10s to achieve a mass flow rate of 1.0 Kg/s, which is maintained constant. The discharge pressure is kept constant and equal to the atmospheric pressure. Air was considered an ideal gas with the gas constant equal to 287 J/(KgK). The temperature was maintained at 294 K and the absolute viscosity  $\mu_f$  was kept constant and equal to 19  $\mu Pa.s$ .

The pig had a mass equal to 5 Kg. The static contact forces were:  $F_{stat} = 1000N$  and  $F_{stat} = 4000N$ , for the pipeline and for the flanges respectively, while the dynamic forces were  $F_{dyn} = 970N$  and  $F_{dyn} = 3950N$  for the pipeline and for the flanges.

In order to obtain solutions not influenced by the time step and grid spacing, time interval and the number of nodes were set to 0.01 s and 100 respectively.

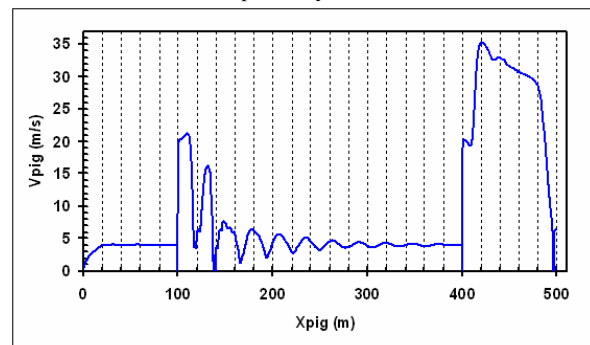
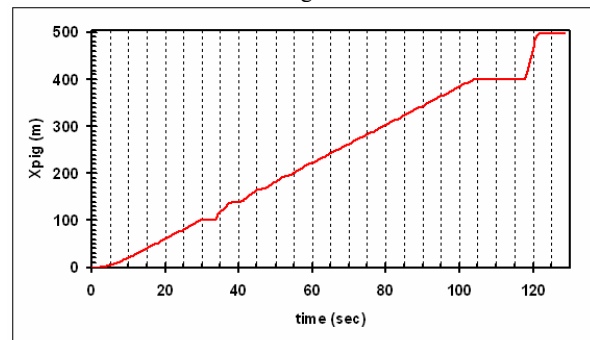
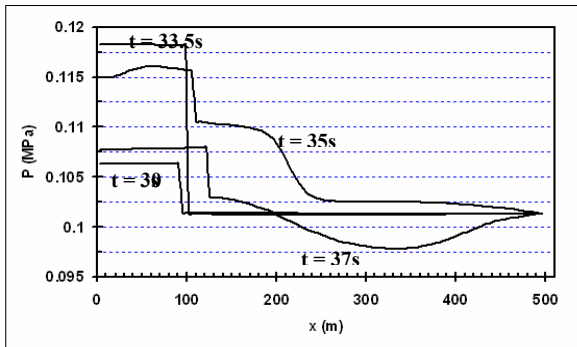


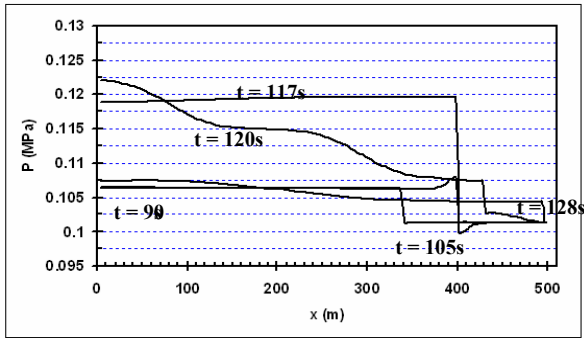
Figure 2. Pig velocity versus pig position for pipeline with flanges



slows down the pig. Before the pig stops, pressure builds up and the pig's velocity increases abruptly, leading to the second expansion of the gas. After the pig stops at  $37.4\text{ s}$ , the pressure builds up again and the pig is driven to the second flange. However, pig's speed increases and decreases until it reaches a steady state value around  $4.0\text{ m/s}$ , which is corresponding to  $1.0\text{ Kg/s}$  mass flow inlet. The pig is, once more, stopped by the higher contact force at the second flange location. Another pressure buildup period is verified ( $104\text{ s} \leq t \leq 118\text{ s}$ ) until the pig overcomes the flange contact force. After released from the second flange, the pig reaches an even higher velocity level, because the volume of pressurized gas upstream of the pig is now higher than when the pig was released from the first flange. As the pig moves along the last section of the pipeline, the upstream gas pressure is seen to decrease.



(a)



(b)

Figure 4. Pressure distribution along pipeline at different time steps; pipeline with flanges

### Pigging with Bypass Pigs in a Pipeline with a Branch

This case consists of an isothermal air flow at  $300\text{ K}$  inside a  $500\text{ m}$  pipeline which has been sketched schematically in Fig. 5. The inlet pressure is maintained constant and equal to  $500\text{ KPa}$ , while the mass flow rate at the exit is imposed. Initially there is no flow in the pipe, increasing linearly with time taking  $20\text{ s}$  to reach  $0.3\text{ Kg/s}$ , and is kept constant. A branch of pipe is considered at  $x = 250\text{ m}$  with a constant mass flow rate of  $0.05\text{ Kg/s}$ . Air is considered ideal with the same properties as "Pigging in a Gas Line with Flanges" case.

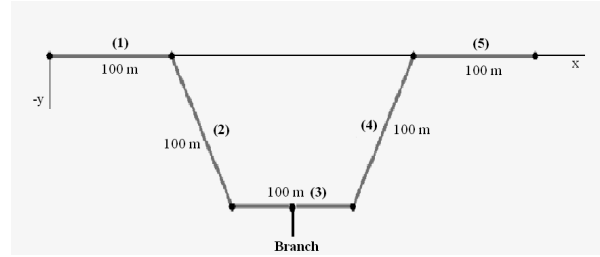


Figure 5. Pipeline schematic

The following data were used in the computations: pipeline diameter:  $0.1\text{ m}$  (other pipe parameters are the same as the previous case), bypass hole area:  $0.0003\text{ m}^2$ , localized pressured drop coefficient at the bypass:  $1.5$ , pig mass:  $3\text{ Kg}$ , static and dynamic contact forces:  $50\text{ N}$  and  $40\text{ N}$ , number of nodes:  $100$ , time interval:  $0.01\text{ s}$ .

Results concerning the pig dynamics, which are presented in Figures 6(a) and (b), show that the pig does not move, while the rising pressure force is not sufficient to overcome the static contact force value. When this value is attained, the pig starts moving with a high acceleration at  $t = 6.25\text{ s}$ . The pig velocity increases by increasing the mass flow rate until it reaches a steady state value around  $6.5\text{ m/s}$ . At  $x = 100\text{ m}$  where the pig enters pipe section (2), the velocity increases due to gravitational acceleration. However, the speed drops again when the pig enters horizontal pipe section (3) at  $x = 200\text{ m}$ . The pig gains its steady speed value of  $6.5\text{ m/s}$  until it reaches the branch pipe. By passing the branch pipe, pig speed decreases abruptly due to pressure drop behind the pig. Under this condition, this velocity reaches its new steady value of  $5.5\text{ m/s}$ . As the pig enters pipe section (4), gravitational force acts in the opposite direction of the pig motion, resulting in a drop in pig velocity. However, by entering the horizontal pipe section (5), the speed rises again to steady value of  $5.5\text{ m/s}$ .

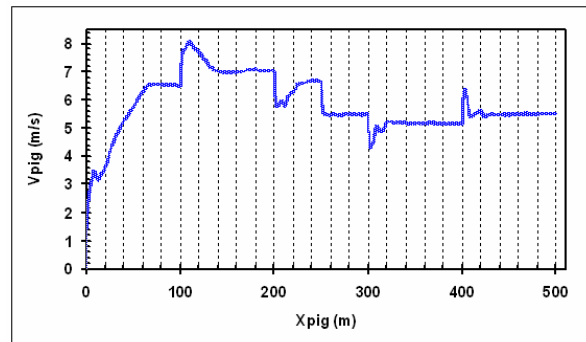


Figure 6(a). Pig velocity versus pig position for pigging with bypass pigs

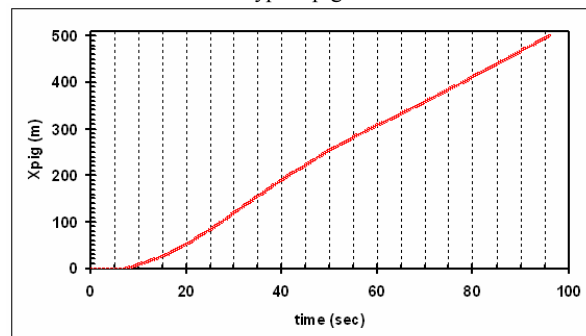


Figure 6(b). Time variation of pig position for pigging with bypass pigs

### Pigging with Bypass Pigs, Comparison of Real and Ideal Gas

In this case, simple pigging simulation with a bypass pig in a 50 meter long horizontal pipe has been considered in order to analyze real and ideal gas effects. Air at high pressure of 9.0 MPa is used as the working fluid. Mass flow rate increases linearly with time from 0.0 to 4.0 Kg/s in 10 s and then kept constant. All other parameters are the same as the previous case.

Results are presented in Fig.7. An observation of this figure shows that there is no significant difference between real and ideal gas solutions. In both cases, pig attains almost the same steady velocity value of 4.6 m/s after 10 s. The traveling time of the pig is 16.37 s for real gas case which is 0.1 s more than the ideal gas case. It should be noted that the computer run time of the program for real gas case is considerably greater than for ideal one. Thus, using real gas mode for pigging simulation is not justified.

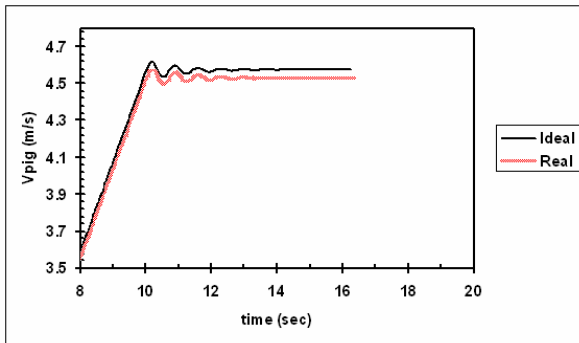


Figure 7. Pig velocity versus pig position, comparison between real and ideal gas

### Conclusions

This paper presented a study aimed at simulating the dynamic behavior of pigs in pipelines driven by gas. The basic equations governing conservation of mass and linear momentum for the fluid were numerically solved, coupled with the linear momentum equation for the pig and models for bypass flow through the pig. The results obtained concerning pig velocity and acceleration, and pressure fields provide a better understanding of the complex behavior of pig motion through pipelines.

### References

- [1] Tiratsoo, J.N.H., *Pipeline Pigging Technology*, Gulf Professional Publishing, 1992.
- [2] Sullivan, J.M., An Analysis of the Motion of Pigs through Natural Gas Pipelines, *Master's thesis, Department of Mechanical Engineering, Rice University*, 1981.
- [3] Haun, R., Analysis and Modeling of Pipeline Dewatering and Startup: Part 1, *Pipeline Industry*, 1986, 37–41.
- [4] Short, G.C., The Pigging Technology Project: The First Three Years, *Pipes & Pipelines Int.*, **39-4**, 1994, 23–27.
- [5] Azevedo, L.F.A., Braga, A.M.B., Nieckele, A.O., Naccache, M.F., and Gomes, M.G.F., Simple Hydrodynamic Models for the Prediction of Pig Motion in Pipelines, *Pipeline Pigging Conference*, Houston, PA, 1995.

- [6] Vianes Campo, E., and Rachid, F.B., Modeling of Pig Motion Under Transient Fluid Flow, *Proc. XIV Brazilian Congress of Mechanical Engineering—COBEM*, Sao Paulo, Brazil, 1997.
- [7] Nieckele, A.O., Braga, A.M.B., Azevedo, L.F.A., Transient Pig Motion through Gas and Liquid Pipelines, *Journal of Energy Resources Technology*, **123**, 2001, 260-269.
- [8] Wylie, E.B., and Streeter, V.L., *Compressible Flow in Pipes*, McGraw-Hill, 1978.
- [9] Fox, R.W., and McDonald, A.T., *Introduction to Fluid Mechanics*, McGraw Hill, 1995.
- [10] Lemmon, E.W., Huber, M.L., McLinden, M.O., *NIST Reference Fluid Thermodynamic and Transport Properties—REFPROP, Version 8.0, User's Guide*, 2007.
- [11] Patankar, S.V., *Numerical Heat Transfer and Fluid Flow*, Hemisphere Publishing Co., 1980.
- [12] Pozrikidis, C., *Numerical Computation in Science and Engineering*, Oxford University Press, 1998.